Chapter 1
Firefly Optimization Based Improved Fuzzy Clustering for CT/MR Image Segmentation

S. N. Kumar, A. Lenin Fred, H. Ajay Kumar and P. Sebastin Varghese

Abstract The segmentation is the process of extraction of the desired region of interest. In medical images, the anatomical organs and anomalies like a tumor, cysts, etc. are of importance for the diagnosis of diseases by physicians for telemedicine applications. The thresholding, region growing, and edge detection are termed as classical segmentation algorithms. Clustering is an unsupervised learning technique to group similar data points and fuzzy partitioning merges similar pixels based on the fuzzy membership value. The classical FCM algorithm lacks sensitivity in the cluster centroid initialization and often gets trapped in local minima. The optimization algorithm gains its importance in cluster centroids initialization, thereby improving the efficiency of FCM algorithm. In this work, firefly optimization is coupled with FCM algorithm for CT/MR medical image segmentation. Fireflies are insects having a natural capacity to illumine in dark with glowing and flickering lights and firefly optimization algorithm was modeled based on its biological traits. The preprocessing stage comprises of artifacts removal and denoising by Nonlinear Tensor Diffusion (NLTD) filter. The computation time was minimized by reducing the total pixels count for the processing. The Firefly optimization, when coupled with FCM, generates satisfactory results inconsistent with FCM when coupled with Cuckoo, Artificial Bee Colony, and Simulated annealing algorithms. The cluster validity performance metrics are used for the determination of optimum number of clusters. The algorithms are developed in Matlab 2010a and tested on real-time abdomen datasets.

S. N. Kumar (✉)
Sathyabama Institute of Science and Technology, Chennai, India
e-mail: appu123kumar@gmail.com

A. Lenin Fred · H. Ajay Kumar
Mar Ephraem College of Engineering and Technology, Elavuvilai, India
e-mail: leninfred.a@gmail.com

H. Ajay Kumar
e-mail: ajayhakkumar@gmail.com

P. Sebastin Varghese
Metro Scans and Research Laboratory, Trivandrum, India
e-mail: sebastin464@gmail.com

J. Hemanth and V. E. Balas (eds.), *Nature Inspired Optimization Techniques for Image Processing Applications*, Intelligent Systems Reference Library 150,
https://doi.org/10.1007/978-3-319-96002-9_1

Keywords Unsupervised learning · Clustering · Fuzzy C means
FCM-firefly algorithm · FCM-artificial bee colony algorithm · FCM-cuckoo algorithm

1.1 Introduction

Medical image processing refers to the application of computer-aided algorithms for the extraction of anatomical organs and analysis of anomalies like a tumor, cyst, etc. The various steps in image processing are restoration, enhancement, segmentation, classification, and compression. The segmentation can be defined as the extraction of Region of Interest (ROI). The Computer Tomography (CT), Magnetic Resonance Imaging (MRI), Ultrasound and Positron Emission Tomography (PET) are the widely used medical imaging modalities for the disease diagnosis. The choice of segmentation algorithm depends on the medical imaging modality and its characteristics.

The CT images, in general, are corrupted by Gaussian noise and its distribution is as follows.

$$p(z) = \frac{1}{\sqrt{2}\pi\sigma} e^{-(x-\mu)^2/2\sigma^2}$$

where x represents random variable normally distributed with mean μ and standard deviation σ.

The MR images are corrupted by rician noise, artifacts and intensity inhomogeneity due to the non-uniform response of RF coil. The rician noise distribution is as follows

$$p(z) = \frac{z}{\sigma^2} \exp\left(-\frac{z^2 + I^2}{2\sigma^2}\right) B\left(\frac{z\alpha}{\sigma^2}\right)$$

where, I is the true intensity value, σ is the standard deviation of the noise, and B is the modified zeroth order Bessel function.

The Ultrasound images, in general, are corrupted by speckle noise and its distribution is as follows.

$$F(x) = \left(\frac{g^{\gamma-1}}{(\gamma-1)!a^{\gamma}} e^{\frac{g}{a}}\right)$$

where, α is the variance, γ is the shape parameter of gamma distribution and g is the gray level.

Prior to segmentation, the preprocessing was performed by appropriate filtering technique; Filter selection is based on the medical imaging modality and noise characteristics. The role of preprocessing is inevitable in signal and image

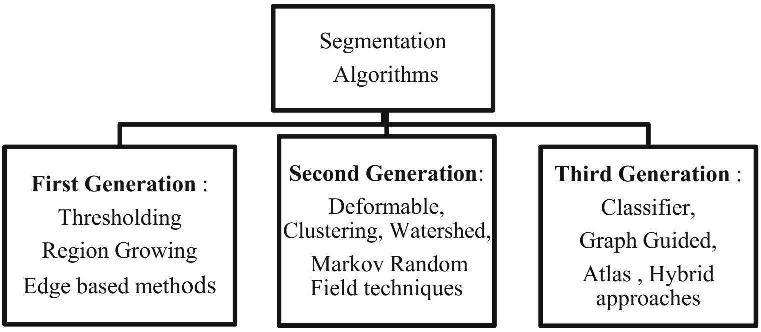

Fig. 1.1 Classification of segmentation algorithms

processing for subsequent operations like segmentation and classification [1, 2]. The segmentation algorithms can be categorized based on the generation of evolution and are depicted in Fig. 1.1.

Image segmentation is the process of grouping the pixels of an image to form meaningful regions. Medical image segmentation is the visualization of the region of interest such as anatomical structures and anomalies like tumor, cyst, etc. for medical applications such as diagnostics, therapeutic planning, and guidance. Lay Khoon Lee et al. performed a review on different types of segmentation algorithms for medical imaging modalities like X-ray, CT, MRI, 3D MRI and Ultrasound [3]. Similarly, S. N. Kumar et al. performed a detailed study on the different generation of the medical image segmentation techniques; qualitative and quantitative analysis was performed for the widely used medical image segmentation algorithms [4]. Neeraj Sharma et al. state the necessity of automated medical image segmentation technique in diagnosis, and radiotherapy planning in medical images and also explained the limitations of the existing segmentation algorithms [5]. The thresholding is a simple and classical technique that separates the foreground and background regions in an image based on the threshold value. The multilevel thresholding eliminates the discrepancy of the bi-level thresholding that uses a single threshold value. The optimization techniques when employed in the multilevel thresholding yield efficient results, since it provides the proper choice of threshold values. The 3D Otsu thresholding was found to be efficient for MR brain images; better results were produced than bi-level and multithresholding techniques [6]. Among the region based approaches, the classical region growing is the semi-automatic segmentation technique that relies on the seed point selection [6]. The multiple-seed point based region growing for brain segmentation was found to be effective on a multi-core CPU computer [7]. The manual seed point selection can be replaced by the deployment of the optimization algorithm for yielding efficient results [8]. The edge detection traces the boundary of objects in an image and among the classical edge detector, canny produces better results [9]. The Markov basics and Laplace filter were coupled to form an edge detection model that gives better results for medical images than the classical techniques [10]. The teaching learning-based optimization was found to be effective for medical image edge detection than the classical edge detectors [11]. The interactive medical image segmentation algorithms are discussed in [12]. J. Senthilnath et al. did a performance study on nature-inspired firefly optimization algorithm in the thirteen benchmark classification datasets [13]. Superior results were produced when compared with classical techniques like Particle Swarm Optimization (PSO), Bayes net, Multilayer Perceptron, Radial Basis Function Neural Network, KStar, Bagging, MultiBoost, Naive Bayes Tree, Ripple Down Rule, Voting Feature Interval.

Iztok Fister et al. made a detailed analysis of the types of firefly algorithm for engineering applications in solving the real world challenges [14]. Hui Wang et al. proposed a modification in the parameter of classical firefly algorithm to reduce the complexity of the algorithm [15]. The proposed adaptive firefly algorithm generates better solution when compared with standard Firefly Algorithm, Variable step size Firefly Algorithm (VSSFA), Wise step strategy Firefly Algorithm (WSSFA), Memetic Firefly Algorithm (MFA), Firefly Algorithm with chaos and Firefly Algorithm with random attraction. Mutasem K et al. proposed a hybrid technique comprising of the Fuzzy C-Means algorithm with Firefly algorithm for the segmentation of brain tumor [16]. The experimental analysis was carried out on 181 brain images obtained from brain-web Simulated Brain Database (SBD) repository; robust results were produced when compared with Dynamic clustering algorithm based on the hybridization of Harmony Search and Fuzzy Variable String Length Genetic Point symmetry techniques. K. Vennila et al. proposed multilevel Otsu image segmentation based on Firefly optimization and good results were obtained in terms of PSNR, computation cost and mean value when compared with Darwinian Particle Swarm Optimization [17]. Cholavendhan Selvaraj et al. made a detailed survey of the bio-inspired optimization algorithms such as Ant Colony Optimization, Particle Swarm optimization, Artificial Bee Colony algorithm and their hybridizations [18].

The summarization of results reflects the status of the optimization techniques in solving the wide range of engineering problems. In the medical image processing, the FCM plays a major role in the clustering and classification of the image for the analysis, diagnosis, and recognition of anomalies [19]. Janmenjoy Nayak et al. performed a survey on major modification and advancement in the classical FCM algorithm and their applications towards the image analysis [20]. Chih Chin Lai et al. proposed a hierarchical evolutionary algorithm based on genetic algorithm for the segmentation of skull images which enhances the diagnostic efficiency than the dynamic thresholding, Competitive Hopfield Neural Networks (CHNN), K-Means and Fuzzy C-Means algorithms [21].

Emrah Hancer et al. proposed a methodology for the segmentation of brain tumor in the MRI images by using artificial bee colony algorithm. Efficient results were produced when compared with K-Means, FCM, and Genetic Algorithm based image segmentation techniques [22]. The FCM, when coupled with PSO was found to be effective for the segmentation of noisy images when compared with K-means, Enhanced FCM, and Fast Global Fuzzy Clustering techniques [23].

The Convolution Neural Network (CNN) was employed for the automatic segmentation of MR brain images, multiple convolution kernels of varying size was used for the generation of accurate results [24]. The CNN with multiple kernels of smaller size was used for the efficient brain tumor segmentation in MR images [25]. The Deep Learning Neural Network (DLNN) gains its importance in attenuation correction of PET/MR images [26]. The DLNN along with deformable model was proposed for the automatic segmentation of left ventricle in cardiac MR images [27]. The Deep Convolution Neural Network (DCNN) along with the 3D deformable model generates good segmentation results for the extraction of tissues in musculoskeletal MR images [28]. Vijay Badrinarayanan et al. proposed SegNet, a novel DCNN architecture for semantic pixel-wise segmentation [29]. In this chapter, firefly optimization algorithm was coupled with FCM for CT/MR medical image segmentation. The preprocessing stage comprises of artifacts removal and denoising by Non-Linear Tensor Diffusion (NLTD) filter. The computation complexity of the algorithm was minimized by sampling the total pixel count for manipulation. The Cluster Validity Indexes (CVI's) are used for the validation of results to determine the optimum number of clusters.

1.2 Materials and Methods

1.2.1 Data Acquisition

The real-time abdomen CT data sets are used in this work for the analysis of algorithms. The images are acquired from Optima CT machine with a slice thickness of 3 mm. The images in DICOM format with a size of 512 × 512 are used in this work. The Metro Scans and Research Laboratory approved the study of human datasets for research purpose. The five abdomen CT data sets, each comprising of 200 slices are used in this work. The results of typical slice from each dataset are depicted here.

1.2.2 Fuzzy C Means Clustering

In this chapter, the Fuzzy c-means Clustering algorithm coupled with optimization technique was proposed for the segmentation of medical images. In the perspective of image processing, clustering is defined as the grouping of pixels into a cluster which is similar between them, while dissimilar pixels belong to other clusters. The concept of clustering is depicted below in Fig. 1.2. The clustering algorithms can be classified into two groups; Supervised and Unsupervised. The requirement of prior knowledge termed as training samples is the key concept of the supervised classifier. Artificial Neural Network (ANN), Naive Bayes Classifier, and Support

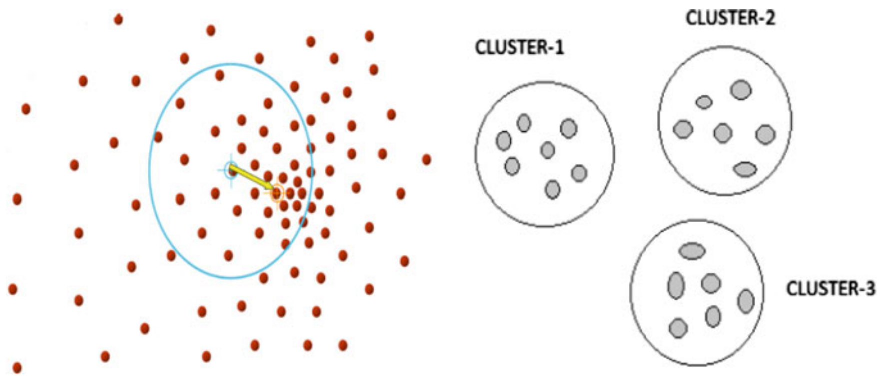

Fig. 1.2 Principle of clustering

Vector Machine are some of the widely used supervised algorithms. The unsupervised technique doesn't need any prior information and is particularly well suited for huge unlabeled datasets. The unsupervised clustering techniques can be further classified into two categories; hierarchical and partitional. The role of partitional clustering is prominent in image analysis and pattern recognition. The K-means and Fuzzy c-means (FCM) are well-known partition clustering algorithms. The K- means clustering is termed as Crisp (hard) since the objects are assigned to only one cluster. The FCM clustering is termed as soft (Fuzzy) since an object can be accommodated in more than one cluster based on the fuzzy membership value.

The FCM overcomes the issues of classical K-means clustering; since the data can belongs to more than one cluster. The FCM was developed by Dunn [30] and modified by Hathaway and Bezdek [31] which was widely used for pattern classification. FCM is an unsupervised algorithm based on the minimization of the objective function.

$$J_m = \sum_{i=1}^{N} \sum_{j=1}^{C} U_{ij}^{m} \left\| y_i - c_j \right\|^2, \quad 1 \leq f < \infty$$

The pixels are grouped into clusters in such a manner that, the intracluster similarity is maximized and the intracluster similarity is minimized.

The fuzzy partition represents the fuzzy membership matrix of the pixel in the cluster. The parameter U_{ij} represents the fuzzy membership of the ith object (pixel) in the jth cluster. The parameter 'f' depicts weighting exponent that determines the degree of fuzziness for the fuzzy membership function. The fuzzy classification is based on the iterative optimization of the objective function depicted above with the updation of membership function u_{ij} and the cluster center c_j as follows.

$$U_{ij} = \frac{1}{\sum_{K=1}^{C}\left(\frac{\left\|y_i - c_j\right\|}{\left\|y_j - c_k\right\|}\right)^{\frac{2}{f-1}}}$$

$$c_j = \frac{\sum_{i=1}^{N} U_{ij}^{f} \cdot y_i}{\sum_{i=1}^{N} U_{ij}^{f}}$$

The iterative calculation is terminated, when $max_{ij}\left\{\left|u_{ij}^{(k+1)} - u_{ij}^{(k)}\right|\right\} < \delta$, where δ is a termination criterion between 0 and 1, and k represents the iteration count. The convergence of the algorithm occurs when the objective function (J_m) attains local minima or saddle point.

The steps in FCM clustering algorithm are summarized as follows

1. *Initialise* $U = [U_{ij}]$ *matrix*, $U^{(0)}$
2. *At* k^{th} *step: Calculate the cluster center vector* $C^{(k)} = [c_j]$ *with* $U^{(k)}$

$$c_j = \frac{\sum_{i=1}^{M} U_{ij}^{m} \cdot x_i}{\sum_{i=1}^{M} U_{ij}^{m}}$$

3. *Update* $U^{(k)}, U^{(k+1)}$

$$U_{ij} = \frac{1}{\sum_{K=1}^{C}\left(\frac{\left\|x_i - c_j\right\|}{\left\|x_j - c_k\right\|}\right)^{\frac{2}{m-1}}}$$

4. *If* $\left\|U^{(k+1)} - U^{(k)}\right\| < \delta$, *then Stop; otherwise return to step* 2.

The operating principle of FCM is based on the fact that, the minimization of the objective function ends up with the solution. In many real-time cases, classical FCM stuck into local minima. The optimization algorithm can be employed to achieve global minima. The parameter selection is vital for optimization algorithms and it influences the performance of the algorithm to maximize or minimize the objective function subjecting to certain constraints. The cluster centers are randomly initialized by classical FCM, hence the optimization based clustering solves this problem. The cluster centers generated by the optimization technique is utilized by the FCM for image segmentation. The pixels in the image are mapped into the particular cluster based on similarity and distance. The initialization of the cluster centers by optimization improves the performance in terms of the convergence rate, computation complexity, and segmentation accuracy.

1.2.3 Firefly Optimization Algorithm

In this chapter, the performance of firefly optimization in the FCM algorithm was analyzed for the estimation of optimal cluster center values for image segmentation. The biological trait of the firefly is the motivation for Yang [32] to propose an optimization technique. The rhythmic flashes generated by the firefly was used as a mode of communication between them to search for prey and for mating. More than 2000 species of fireflies are there in the world and they have natural characteristics to create illumination in the dark with flickering and glowing lights. Fister et al. found that the attraction capacity of the fireflies is proportional to the brightness [14]. The fireflies tend to move towards ones which emits a brighter light.

The population-based firefly algorithm was found to generate a global optimal solution for many engineering problems. The biological chemical substance luciferin present in the body of the fireflies was responsible for flashing the light. The intensity of light emitted is directly proportional to the discharge of luciferin. The degree of attraction tends to decrease as the distance between the fireflies increases. If any firefly fails to discover another firefly which is brighter than itself, it will travel arbitrarily. The optimization algorithm when employed for clustering applications, cluster centers are the decision variables and the objective function is associated with the euclidean distance. Based on the objective function, initially, all the fireflies will be spread randomly over the search space.

The two stages of firefly algorithm are summarized as follows:

The first stage is based on the difference in the intensity that is associated with the objective function values. Depending on the nature of the problem that requires maximization/minimization, a firefly with higher/lower intensity will entice another individual with higher/lower intensity.

Consider that there are n swarms (fireflies), where Y_i signifies the solution of a firefly i. The fitness value is expressed by $f(Y_i)$ moreover the current position I of the fitness value $f(y)$ is estimated by the brightness of a firefly [32].

$$I_i = f(y_i), \quad 1 \leq i \leq n$$

The second stage is the movement towards the firefly with high brightness intensity. The attraction factor of the firefly is represented by β that indicates the attraction power of firefly in the swarm and it changes with distance (R_{ij}) between two fireflies i and j at positions Y_i and Y_j respectively.

$$R_{ij} = \left\|Y_i - Y_j\right\| = \sqrt{\sum\nolimits_{k=1}^{d} \left(Y_{ik} - Y_{jk}\right)^2}$$

The attraction function $\beta(R)$ of the firefly is expressed as follows.

$$\beta(R) = \beta_0 e^{-\gamma R^2}$$

where β_0 is the attraction function value for $R = 0$, γ is the coefficient of ingestion of light.

The pseudo code for firefly optimization algorithm is as follows

```
Define objective function f(Y), Y=[Y1,Y2,Y3,--------Yd]

Generate initial population of fireflies Yi =[1,2,3-----n]

Estimate the light intensity of firefly Ii using the objective function  f(Y)

 Define light absorption coefficient(γ)

While (t<max generation )

        for i=1:n    //all n fireflies

            for j=1: n   // all n fireflies

                      if (Ij > Ii)

                            Move firefly i towards j in d dimensions.

             end if

                                  // Attraction capacity changes with distance

                                  //Validate new solutions and update light intensity

         end for j

                  end for i

Estimate the current best by ranking the fireflies

end while
```

The motion of a firefly ‘i’ from the position Y_i which is attracted towards another brighter firefly ‘j’ at position Y_j is expressed as follows

$$Y_i(t+1) = Y_i(t) + \beta(R)\left(Y_i - Y_j\right) + \alpha\left(rand - \frac{1}{2}\right)$$
$$Y_i(t+1) = Y_i(t) + \beta_0 e^{-\gamma R^2}\left(Y_i - Y_j\right) + \alpha\left(rand - \frac{1}{2}\right)$$

where α depicts the maximum radius of the random step. The term rand represents randomization parameter uniformly distributed between 0 and 1.

There are two special cases

Case i: $r = 0$, then $\beta = \beta_0 e^0 = \beta_0$, The air is absolutely clear with no light dispersion. The fireflies can see each other; exploration and exploitation is out of balance.

Case ii: $r = \infty$, then $\beta = I_0 e^{-\infty d^2} = 0$, The air is foggy with extreme light dispersion. The fireflies can't see each other; exploration and exploitation is out of balance.

1.2.4 Improved FCM-Firefly Optimization Segmentation Algorithm

The FCM clustering algorithm proposed here comprises of two stages. In the first stage, firefly optimization is employed to determine the near-optimal cluster centers. In the second stage, the cluster centers are used for the initialization of FCM algorithm. The firefly optimization algorithm makes the clustering an effective tool for medical image segmentation by eliminating the problem of stucking at local minima. The firefly optimization is a swarm intelligence based algorithm and hence it mimics its advantages.

The solution vector is expressed as follows

$$S = \begin{pmatrix} V_1 & V_2 & V_3 \\ S_1, S_2, \ldots, S_i \ldots S_d & S_1, S_2, \ldots, S_i \ldots S_d & S_1, S_2, \ldots, S_i \ldots S_d \end{pmatrix}$$

where S_i represents characteristics in numerical form such that S_i € S. The 'S' depicts the array representing pixel attribute. Each cluster center V_i is represented by d numerical features $(S_1, S_2, \ldots S_d)$. Each solution vector is of the size (c $\times$ d), where c indicates given number of clusters and d represents the features of the dataset.

For the delineation of anomalies like tumor or cyst or anatomical organs, each pixel in the image is mapped into the clustering sector. The cluster centers are randomly initialized from the image pixel gray values with the randomly initialized solution vector, the fitness value is determined by the objective function. The solution vector is then rearranged based on the decreasing order of the objective function value. The firefly optimization determines near optimal cluster centers thereby ensuring global minima for FCM algorithm and hence eliminates the trapping at local minima. The improved FCM based on firefly optimization replaces the classical techniques of random initialization.

Prior to filtering, the medical image film artifacts are eliminated by a statistical technique coupled with convex hull computational geometry [33]. The threshold value determined by standard deviation technique was used for the binarization of input image. The binarized image was then subjected to connected component labeling for the elimination of patient details and technical information. The convex hull of the resultant image was multiplied with the original image for the generation of artifacts removed image. The preprocessing of input image was performed by Non-Linear Tensor Diffusion (NLTD) filter prior to segmentation [34]. The NLTD ensures good edge preservation since the smoothing is heterogeneous and non-noisy pixels are not disturbed.

The computation complexity was minimized by reducing the pixel count for the processing by segmentation algorithm.

$$Rp = randperm\,(L)$$

The parameter S_p represents the pixels taken for optimization, here in this work 50% of the total pixels are taken. The L represents the total pixel count of the image to be segmented and randperm function returns a row vector depicting a random permutation of the integers from 1 to n.

$$S_n = ceil\left(L * S_p\right)$$

The S_n represents the number of pixels selected for optimization and the function below represents the subset of pixels chosen for optimization process

$$X_2 = X(Rp(1 : S_n), :)$$

The optimization of the objective function relies on the brightness and movements of the firefly. The firefly algorithm starts by initializing the population of fireflies. The intensity of light emitted by the firefly estimates the movement of the fireflies. The algorithm works in the iterative fashion. The intensity of ith firefly is compared with the jth firefly as follows

if $\beta(i) > \beta(j)$
firefly j move towards firefly i
else
firefly i move towards firefly j

The incorporation of firefly algorithm has significantly improved the segmentation results. There were four stages of Improved FCM-Firefly segmentation algorithm.

i. Initialization phase
ii. Intensity calculation phase
iii. Movement calculation phase
iv. FCM algorithm phase.

The goal of incorporating firefly optimization in FCM is to minimize the objective function with a global minima value. The cluster centers represent the decision parameters to minimize the objective function. The initialization of the firefly population is as follows

$$y_{if} = \left[y_{i1}, y_{i2}, \ldots, y_{ij}, \ldots y_{id}\right] \quad 2 < j < C$$

Each firefly in the population is represented by using the above equation. Where y_{ij} represents the jth cluster centre.

The population of the fireflies are initialized and randomly distributed in search space. The position of firefly depicts the possible solution (centroids) for the clustering problem. In this phase, the parameter like β_0, γ, α and maximization iteration are also initialized. Once the initialization process is over, the intensity of each firefly is determined by estimating the distance between the position of the firefly and the entire data in the dataset. The minimum distance value among the population with respect to data from the dataset is considered. The intensity value of each firefly is determined based on the sum of minimum distance with respect to the data from the dataset.

The expression for determination of intensity is as follows

$$\beta(FF_j) = \sum_{i=1}^{n} d_i$$

where FF represents firefly, d_i represents the minimum distance value for a particular firefly.

The brightness of the fireflies indicates the movement of the fireflies in the search space. The intensity of fireflies is compared to determine the new position. The difference in the brightness triggers the movement. The firefly optimization is employed in the FCM algorithm to enhance the clustering operation. The new position of the entire swarm of the fireflies is determined by the FCM operator based on the current intensity value.

The FCM-Firefly algorithm is carried out through the updation of the membership value u_{ij} and position of the firefly y_j using the below equations

$$U_{ij} = \frac{1}{\sum_{k=1}^{s}\left(\frac{\|y_i - f_j\|}{\|y_i - f_k\|}\right)^{2/f-1}}, \quad 1 \le i \le N$$

where U_{ij} depicts the degree of membership of y_i in the firefly j, degree of fuzziness f = 2 and y_i is the data associated with the firefly under study.

$$F_j = \frac{\sum_{i=1}^{N} u_{ij}^{m} \cdot x_i}{\sum_{i=1}^{N} u_{ij}^{m}}$$

The F_j represents the solution after applying FCM in the firefly j.

The new position of Firefly is determined and the intensity value is updated. The fixed number of iterations will be provided and at the end of the iteration, the best solution was determined.

1.3 Results and Discussion

The algorithms are developed in Matlab 2010a and tested on CT abdomen data sets. The system specifications are as follows; Intel Core i3 processor of 3.30 GHz with 4 GB RAM. In the scenario of medical image segmentation, fixing the number of clusters is cumbersome, since it cannot be initialized roughly by viewing the image. The validation metrics are employed for the optimal cluster selection.

This is performed in 3 steps

i. The parameters of clustering algorithm except the cluster number is fixed.
ii. The cluster number is varied from an initial value of 2 to an upper limit (max). The data partition is carried out for each cluster number.
iii. The cluster validity indexes are applied on the data partition obtained from the previous stage for evaluation. Based on the values of CVI's, the cluster number selection is done.

The terminologies used in the formulation of cluster validity function are as follows

N: the count of data objects for clustering
f: the fuzzifier factor that represents the level of cluster fuzziness
u: the ith data object, $1 \le i \le N$
P: the number of clusters
C_p: the pth cluster, $1 \le p \le P$
$|C_p|$: the count of data objects in the p-th cluster
V_p: the centroid of the p-th cluster
$\|u - v\|$: the distance between a pair of data objects
μ_{ip}: the membership degree of u_i corresponding to C_p.

The FCM algorithm is an iterative technique in which the pixels are grouped into a cluster based on the membership degree through the minimization of the objective function.

$$\sum_{i=1}^{M}\sum_{p=1}^{P}\mu_{ip}^{f}\left\|u_i - V_p\right\|^2, \quad f \geq 1$$

The number of the cluster is taken initially P and randomly P centroids are selected. The objective function represented above is optimized in an iterative fashion by the updation of μ_{ip} and V_p as follows

$$\mu_{ip} = \frac{1}{\sum_{j=1}^{P}\left(\frac{\left\|u_i - v_p\right\|^2}{\left\|u_j - v_c\right\|^2}\right)^{\frac{2}{f-1}}}$$

$$V_p = \frac{\sum_{i=1}^{N}\mu_{ip}^{f}u_i}{\sum_{i=1}^{N}\mu_{ip}^{f}}$$

The iteration terminates when, $\|U_{T+1} - U_T\| < \in$, where $U_T = \left[\mu_{ip}\right]$ represents the matrix comprising of all $\mu_{ik}{}'s$. T is the number of iteration and $\in$ is a threshold specified by the user. The clustering validity metrics are used to estimate the quality of clustering result. The partition coefficient (PC) and partition entropy (PE) is based only on the membership values of fuzzy partition dataset. The criteria for optimum cluster number selection is the maximization of (PC) or minimum of PE. The issues in the performance metrics, PC or PE is that they do not consider the geometrical properties of the dataset.

Xie Beni's index (XBI) and Fukuyama's and Sugeno's index (FSI) are also widely used classical CVI's. XBI and FSI focus on the characteristics, compactness, and separation. The numerical part of the expression XBI in Table 1.1 represents the compactness of fuzzy partition, the denominator part represents the strength of separation between the cluster for optimal clustering. The value of XBI should be minimized for optimum cluster number selection. The expression for FSI in Table 1.1 comprises of two terms. The first term represents the compactness measure and the second term represents separation measure. Though FSI and XBI consider the inter-cluster information, geometrical properties are not considered.

The DB index was obtained by the mean of cluster similarities. For each cluster P, the similarity between P and all other clusters are determined. The term Sp is represented as follows

$$Sp = \frac{1}{|C_P|}\sum_{U_i \in C_p}\left\|U_i - V_p\right\|^2$$

Table 1.1 Classical clustering validation metrics

Cluster validity index	Formula
Partition coefficient (PC) [35, 36]	$PC = \frac{1}{N}\sum_{p=1}^{P}\sum_{i=1}^{N}\mu_{ip}^{2}$
Partition entropy (PE) [35, 36]	$PE(K) = \frac{1}{N}\sum_{p=1}^{P}\sum_{i=1}^{N}\mu_{ip}\log_2\left(\mu_{ip}\right)$
Xie and Beni index (XBI) [37]	$XBI(K) = \frac{\sum_{p=1}^{P}\sum_{i=1}^{N}\mu_{ip}^{2}\left\Vert u_i - v_p\right\Vert^2}{N\cdot\min_{i\neq j}\left\Vert v_i - v_j\right\Vert^2}$
The Fukuyama and Sugeno Index (FSI) [37]	$FSI(K) = \sum_{p=1}^{P}\sum_{i=1}^{N}\mu_{ip}^{f}\left\Vert u_i - v_p\right\Vert^2 - \sum_{p=1}^{P}\sum_{i=1}^{N}\mu_{ip}^{f}\left\Vert v_p - \hat{v}\right\Vert^2$

Table 1.2 Clustering validation metrics based on compactness and separation ratio

Cluster validity index	Formula
Calinski-Harabasz index (CHI) [38]	$CHI(K) = \frac{B_P}{P-1} / \frac{W_p}{N-P}$
Silhouette coefficient index (SCI) [38]	$SCI(P) = SC_1(P) - SC_2(P)$
Centroid similarity index (CSI) [38]	$CSI(K) = \frac{\sum_{p=1}^{P}\left(\frac{1}{\lvert C_P\rvert}\left(\sum_{u_j\in C_P}\max_{u_j \in C_p}\left\Vert u_j - u_i\right\Vert\right)\right)}{\sum_{j=1}^{P}\min_{i\neq j}\left\Vert v_i - v_j\right\Vert}$
Davies Bouldin index (DBI) [38]	$DBI = \frac{1}{P}\sum_{P=1}^{P}\max\frac{S_j + S_p}{\left\Vert V_j - V_p\right\Vert}$
Partition coefficient and exponential separation index (PCAESI) [38]	$PCAESI = \sum_{P=1}^{P}\sum_{i=1}^{N}\frac{\mu_{iP}{}^{2}}{\mu_M} - \exp\left(\frac{-\min_{h\neq p}\left\Vert V_p - V_h\right\Vert^2}{\beta_T}\right)$
Pakhira-Bandyopadhyay-Maulik index (PBMFI) [39]	$PBMFI = \frac{\max_{j\neq lp}\left\{\left\Vert V_j - V_p\right\Vert\right\}\times\sum_{i=1}^{N}\mu_{il}\left\Vert U_i - V_l\right\Vert}{P\sum_{P=1}^{P}\sum_{i=1}^{N}\mu_{iK}^{f}\left\Vert U_i - V_K\right\Vert}$
WL index (WLI) [38]	$WLI = \sum_{P=1}^{P}\sum_{i=1}^{N}\frac{\mu_{ilP}{}^{2}\left\Vert U_i - V_P\right\Vert^2}{\sum_{i=1}^{N}\mu_{iP}}$

Table 1.2 represents the clustering validity metrics based on compactness and separation ratio.

The shortcoming of the traditional CVI's is that they are focusing only on the distance between the cluster centroids. The classical clustering validity indexes were not found to be good for large cluster numbers.

The CS index is a function of the cluster diameter and the mean distance between the cluster centers. The PCAES index is a function of exponential separation component, and normalized partition coefficient.

The CH index is based on the mean between and within the sum of squares. The terms in the CH index are represented as follows

$$B_P = \sum_{p=1}^{P} |C_P| \, \|v_P - \overline{v}\|^2$$

$$W_P = \sum_{p=1}^{P} \sum_{U_i \in C_P} \left\| u_i - v_p \right\|^2$$

The SC index is based on the combination of two functions and evaluates the compactness-separation ratio. The terms in the SC index are represented as follows

$$SC_1(P) = \frac{\frac{1}{P}\sum_{p=1}^{P} \left\| v_p - \overline{v} \right\|^2}{\sum_{p=1}^{P} \left(\sum_{i=1}^{N} \mu_{ip}^{m} \left\| u_i - v_p \right\|^2 / \sum_{i=1}^{N} \mu_{ip} \right)}$$

$$SC_2(P) = \frac{\sum_{p=1}^{P-1} \sum_{j=p+1}^{P} \left(\sum_{i=1}^{N} \left(\min\left(\mu_{ip}, \mu_{ij}\right)^2 \right) / n_{ij} \right)}{\left(\sum_{i=1}^{N} \max\limits_{1 \leq p \leq P} \mu_{ip}^2 \right) / \left(\sum_{i=1}^{N} \max\limits_{1 \leq p \leq P} \mu_{ip} \right)}$$

where SC_1 is related with the geometric properties of data; SC_2 is related with the membership degree properties.

The PBMF index is based on the compactness within clusters and a large separation between clusters. The WL index estimates the compactness of clusters by taking into account fuzzy weighted distance and the fuzzy cardinality of clusters. The five abdomen medical data sets are used for the analysis of algorithms. The cluster number was changed from P = 2 to 6 and for each cluster number, 10 times the executions are done and the performance metrics are validated.

The expression for μ_M and β_T in PCAES index are as follows

$$\mu_M = \min_{1 \leq p \leq P} \left\{ \sum_{i=1}^{N} \mu_{iP}^2 \right\}$$

$$\beta_T = \frac{1}{P} \sum_{P=1}^{P} \left\| V_p - \bar{V} \right\|^2$$

The performance metrics of the first run for the data set (ID1) is represented below in Table 1.3. Each cluster validity metric was represented with ± sign, the "+" indicates that the CVI value should be high and "−" sign indicates that the CVI value should be low. The representative input images corresponding to data sets (ID1 to ID5) after the removal of artifacts are depicted in Fig. 1.3. Figure 1.4 represents the NLTD filtering result. Compared with classical filters like median filter, Gaussian filter, and bilateral filter, the NLTD filter generates efficient result. In the median filter, the noise-free pixels are also affected. The edge preservation is poor in Gaussian and bilateral filter. The performance of Anisotropic Diffusion Filter (ADF) was clearly stated in [40]. The NLTD filter is an improved version of ADF, thereby providing promising restoration results. The FCM results when

Table 1.3 Cluster validity performance metrics values of ID1 in the first run

Cluster validity index	P = 2	P = 3	P = 4	P = 5	P = 6
PC+	0.9119	0.9130	**0.9160**	0.8940	0.8946
PE−	0.2164	0.2240	**0.1989**	0.2703	0.2692
CHI+	8512.6035	8541.22	**8652.3935**	7300.4416	7520.1463
DBI+	0.2027	**0.2107**	0.1619	0.1870	0.1793
XBI+	0.0157	0.0227	**0.0321**	0.0148	0.0125
FSI+	**−108.7419**	−216.2876	−249.4163	−262.5782	−266.6921
SCI+	1.3704	2.6804	**4.8570**	3.7541	4.7213
CSI−	**3.5026**	6.7195	11.7389	16.2443	22.5481
PCAES+	15,264.6105	15,633.7410	**15,846.0836**	15,739.2628	15,684.7342
PBMF+	0.1536	0.1220	**0.1719**	0.1597	0.1393
WLI−	0.0240	0.0154	0.0134	**0.0117**	0.0098

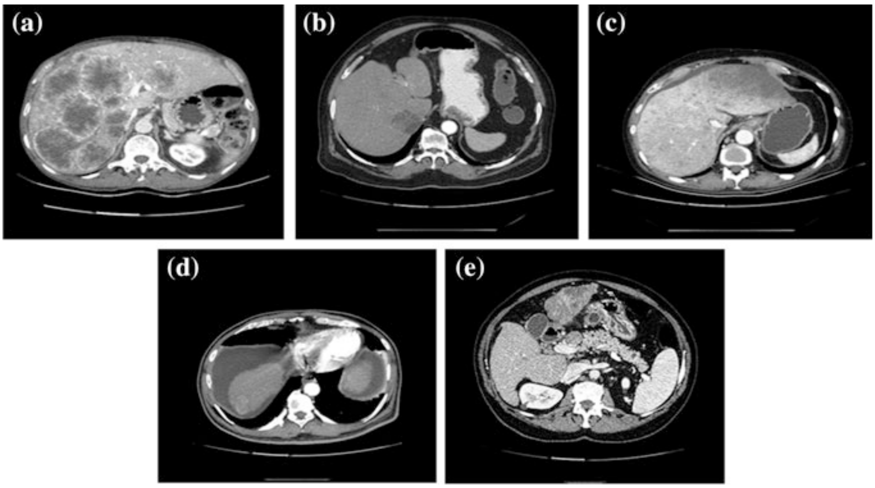

Fig. 1.3 Input images corresponding to five data sets (ID1, ID2, ID3, ID4, and ID5) after the removal of artifacts

coupled with ABC, Cuckoo, SA and Firefly algorithms for a typical slice from the dataset (ID1) are depicted in Fig. 1.5. Figure 1.6 represents the firefly algorithm results for the typical slice from datasets (ID2, ID3, ID4, and ID5). The cluster number selection for the input images is determined from the analysis of CVI's values.

The artifacts removed image was subjected to NLTD filter. The parameters of NLTD filter are step size ($\lambda = 0.24$), diffusion constant ($K = 0.1$) and number of iterations (iter = 10). The Gaussian smoothed image was used for the estimation of

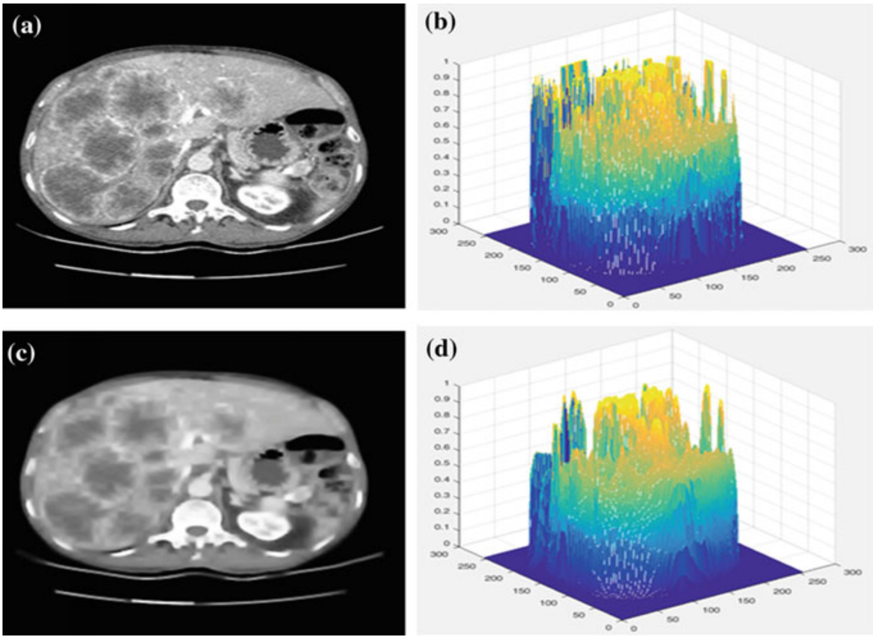

Fig. 1.4 **a**, **b** Artifacts removed image and its color map. **c**, **d** NLTD filter output and its color map corresponding to an input image from dataset (ID1)

conduction coefficient and the elements of the tensor matrix are functions of Gaussian smoothed image components.

The performance metrics are calculated by executing the algorithms 10 times for the images from each data set and the cluster number count are determined. Table 1.8 represents the parameters of optimization algorithms used in this work.

The bold values in Tables 1.3, 1.4, 1.5, 1.6 and 1.7 represents the appropriate value of CVI's in the first run. In Cuckoo, Firefly and ABC optimization, the population (N_p) was set to 20 and the number of iterations was also initialized to 20. Table 1.9 depicts the cluster number count by improved FCM firefly algorithm for 10 runs. For each metric, the cluster count was determined and by the majority voting system, for each metric the optimal cluster number was determined and tabulated in Table 1.10.

The Simulated Annealing was found to be efficient than GA when coupled with FCM, however, the setting of initial temperature is crucial in SA algorithm since it will generate erroneous results [41]. The ABC–FCM yield efficient results than GA-FCM and PSO-FCM in terms of computation time, convergence rate and accuracy [42]. The number of parameters to be tuned is less in cuckoo optimization when compared with the ABC, PSO and GA algorithms. The number of parameters to be tuned for GA and PSO were 4, 6 respectively [43]. The firefly algorithm was found to be efficient for image enhancement when compared with cuckoo optimization in terms of robustness, fitness function and convergence rate [44]. In [45],

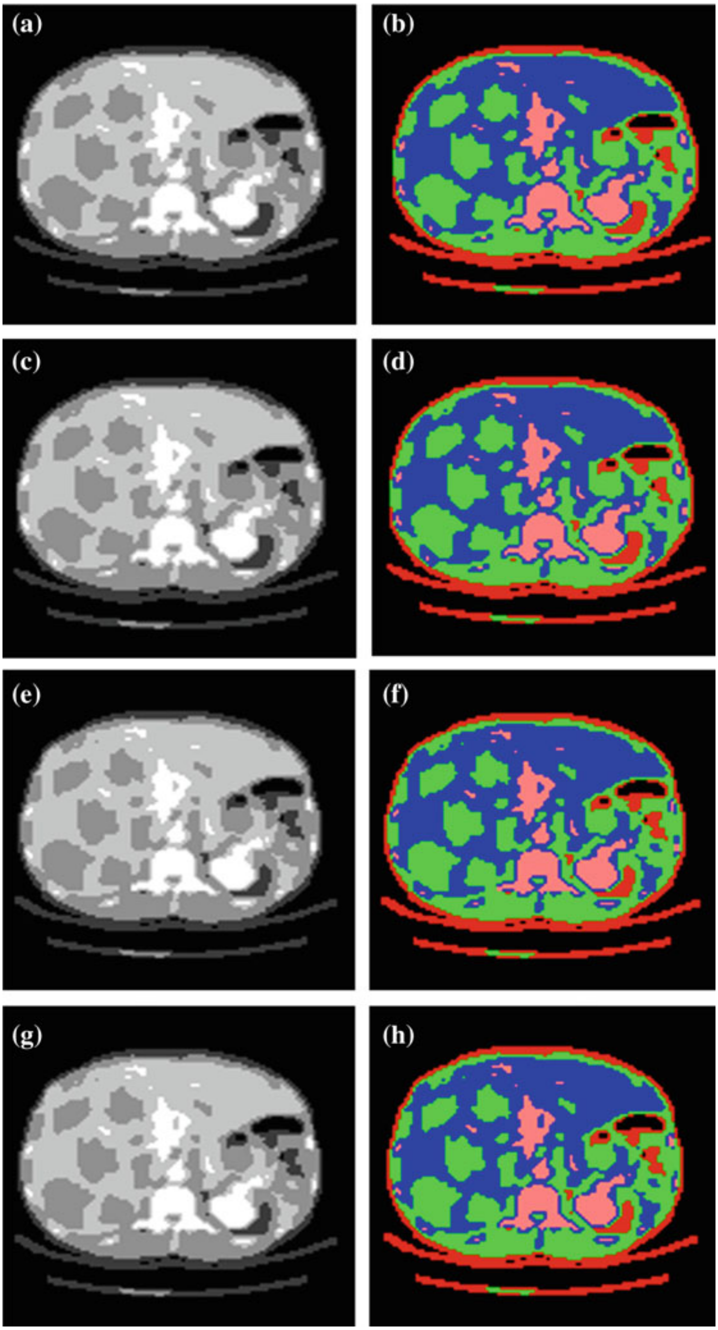

Fig. 1.5 Segmentation results of ID1 **a**, **b** ABC-FCM, **b**, **c** cuckoo-FCM, **d**, **e** simulated annealing-FCM, and **f**, **g** firefly-FCM corresponding to cluster number value of 4

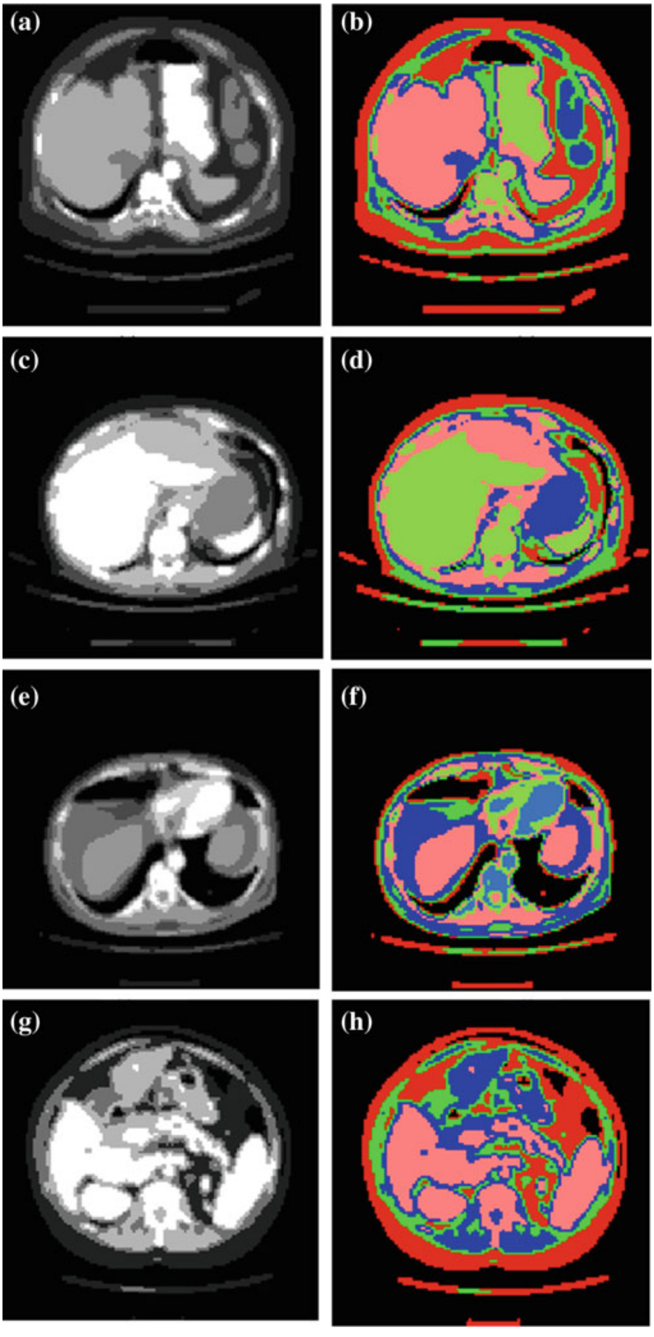

Fig. 1.6 Firefly-FCM segmentation results of ID2 (**a**, **b**), ID3 (**c**, **d**), ID4 (**e**, **f**), ID5 (**g**, **h**) for cluster values 5, 5, 6, 4

Table 1.4 Cluster validity performance metrics values of ID2 in the first run

Cluster validity index	C = 2	C = 3	C = 4	C = 5	C = 6
PC+	0.9218	0.9285	0.9462	**0.9491**	0.9192
PE−	0.1353	0.1997	0.1794	**0.1239**	0.2062
CHI+	**20,575.164**	14,329.983	13,451.709	10,958.149	11,552.368
DBI+	0.1131	0.1379	0.1577	**0.1673**	0.1595
XBI+	0.0122	0.0130	0.0152	**0.0269**	0.0094
FSI+	−416.1045	−406.7087	−402.6203	−364.536	**−254.7033**
SCI+	1.5489	5.7416	6.4141	8.2199	**8.8638**
CSI−	**2.7142**	8.8507	12.2696	25.4724	28.7029
PCAES+	16,991.165	17,193.821	17,115.650	**17,373.889**	17,076.531
PBMF+	0.2229	**0.3725**	0.3053	0.3252	0.2768
WLI−	0.0237	0.0144	0.0106	0.0092	**0.0075**

Table 1.5 Cluster validity index's values of ID3 in the first run

Cluster validity index	C = 2	C = 3	C = 4	C = 5	C = 6
PC+	0.9032	0.9296	0.9339	**0.9350**	0.8975
PE−	0.1952	0.1815	0.1652	**0.1570**	0.2600
CHI+	9406.4576	9366.5511	11,069.808	11,442.9662	**15,577.7010**
DBI+	0.1419	0.1354	0.1551	**0.2354**	0.2278
XBI+	**0.0280**	0.0165	0.0148	0.0203	0.0132
FSI+	−374.5702	−397.8660	**−265.7651**	−392.2532	−395.9922
SCI+	1.8105	3.6604	4.2628	5.0546	**6.8118**
CSI−	**2.2733**	4.6216	8.0308	13.2241	18.5982
PCAES+	13,458.899	13,645.782	13,693.402	**13,832.283**	13,766.516
PBMF+	0.2256	**0.2590**	0.2010	0.2456	0.1286
WLI−	0.0260	0.0144	0.0109	0.0100	**0.0080**

a comparison of Firefly, Bat and Cuckoo optimization was performed; experimental results reveal that firefly outperforms bat and cuckoo algorithm. The tuning of parameters is simple in firefly optimization.

The parameter study reveals that $\beta_0 = 1$ can be used for most of the applications [46]. The studies indicate that the Accelerated PSO [46] is a special case of firefly with $\gamma = 0$. The merits of firefly optimization algorithm are automatic subcategory of population and the capacity to deal with multimodality (Fig. 1.7).

Table 1.6 Cluster validity index's values of ID4 in the first run

Cluster validity index	C = 2	C = 3	C = 4	C = 5	C = 6
PC +	0.9120	**0.9152**	0.9149	0.8909	0.9027
PE−	0.2169	**0.2140**	0.2142	0.2781	0.2473
CHI +	**8509.6424**	5277.0495	6468.0569	5454.4758	5443.1152
DBI +	0.1634	0.1636	0.1533	0.1904	**0.2633**
XBI +	0.0232	0.0198	0.0173	**0.0430**	0.0111
FSI +	−237.1674	−232.2133	−232.2133	−197.3121	**−87.2592**
SCI +	0.8770	2.9675	3.9067	3.6105	**6.8062**
CSI−	20.0393	12.2458	8.9944	5.9863	**2.9196**
PCAES+	10,066.8628	10,350.1937	10,614.0788	**10,714.7197**	10,412.3122
PBMF+	0.1487	0.1843	0.1843	0.2248	**0.2550**
WLI−	0.0354	0.0214	0.0150	0.0135	**0.0098**

Table 1.7 Cluster validity index's values of ID5 in the first run

Cluster validity index	C = 2	C = 3	C = 4	C = 5	C = 6
PC+	0.9297	0.9128	**0.9397**	0.9155	0.9177
PE−	0.2213	0.1760	**0.1440**	0.2131	0.2094
CHI+	12,878.1624	**18,625.8092**	11,641.9111	11,420.381	11,654.719
DBI+	0.1344	0.1612	**0.1749**	0.1507	0.1474
XBI+	0.0168	0.0200	**0.0292**	0.0123	0.0097
FSI+	−571.2952	−561.8331	−532.6463	−506.1773	**−378.2250**
SCI+	1.8957	3.2453	3.6688	6.5740	**7.9765**
CSI−	7.8721	4.6173	**2.1393**	13.1834	17.4610
PCAES+	15,227.6157	15,314.8496	15,075.6335	15,246.377	**15,491.691**
PBMF+	0.2759	0.2510	0.2255	**0.2925**	0.1876
WLI−	0.0300	0.0190	0.0152	0.0109	**0.0085**

Table 1.10 depicts the cluster count manipulated from the CVI's. Table 1.11 represents the optimal cluster value for each dataset determined from the analysis of CVI's.

Table 1.8 Parameters of optimization algorithm

Sl. No.	Optimization algorithm	Parameters
1	Simulated annealing	Initial temperature (T_o): 500 Number of iterations: 250 Cooling schedule (α): 0.4
2	Artificial bee colony	Pheromone evaporation parameter (ρ) [−1 1]: 1 Stagnation limit (L): 10 No. of employed bees [10–30% of total population]: 0.20 * N_p
3	Cuckoo	Step size (α): 1 Levy distribution coefficient(λ) [$1 \leq \lambda \leq 3$]: 1.5 Discovery rate of alien eggs (P_α): 0.25
4	Firefly	Attractiveness coefficient (β_0): 1 Coefficient of ingestion of light (γ): 1 Step size (α): 0.25

Table 1.9 Cluster number count by the improved FCM-firefly algorithm for 10 runs

Data set ID	PC^+	PE^-	CHI^+	DBI^-	XBI^-	FSI^-	SCI^+	CSI^-	$PCAES^+$	$PBMF^+$	WLI^-
1	4^6 3^4	4^6 3^4	4^7 3^3	3^8 4^2	4^8 3^2	2^6 3^4	4^8 3^2	2^8 3^2	4^7 3^3	4^8 3^2	5^5 4^3 3^2
2	5^6 4^4	5^6 4^4	2^3 4^3 5^4	5^8 4^2	5^6 4^4	6^4 5^6	6^8 5^2	2^6 3^4	5^6 4^2 3^2	3^6 5^4	6^4 5^6
3	5^6 6^4	5^6 6^4	6^4 5^3 4^3	5^6 6^3 4^1	2^2 5^3 6^5	5^5 4^3 3^2	6^4 5^3 3^3	2^4 5^6	5^8 4^2	5^6 3^4	6^8 5^2
4	6^6 2^2 5^2	3^2 6^6 5^2	2^2 3^6 6^2	6^8 5^2	5^8 6^2	6^8 5^2	6^8 5^2	6^8 4^1 5^1	5^6 6^4	6^6 4^1 5^3	6^7 5^3
5	4^8 3^2	4^8 3^2	3^6 4^4	4^6 3^4	4^7 3^3	6^6 4^4	6^5 4^4 5^1	4^7 3^3	6^3 5^6 4^1	5^8 4^2	6^6 4^4

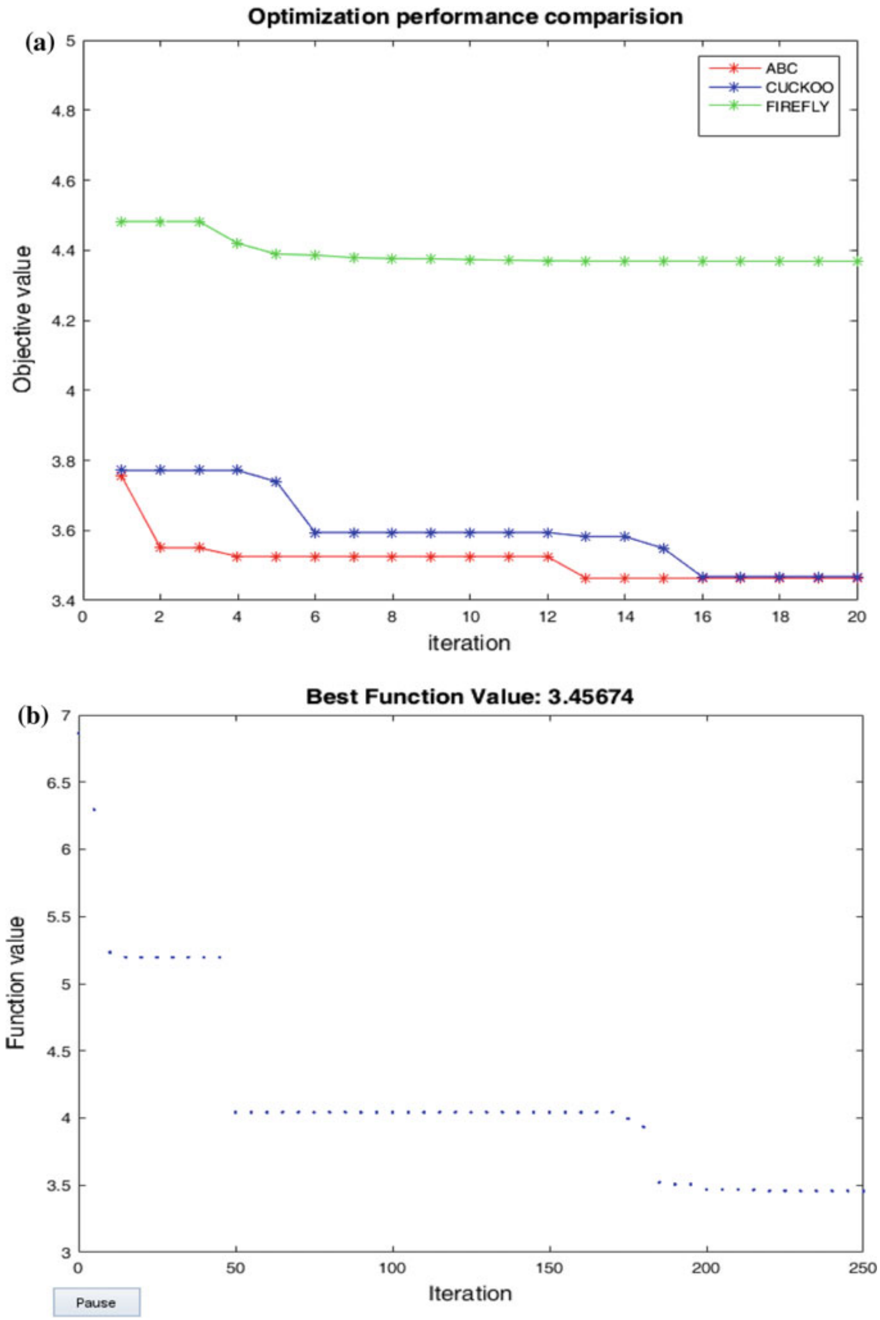

Fig. 1.7 Optimization algorithms performance of ID1: **a** ABC-FCM, cuckoo-FCM and firefly-FCM, **b** SA-FCM

Table 1.10 Possible cluster number decided by CVI's

Data set ID	PC^+	PE^-	CHI^+	DBI^-	XBI^-	FSI^-	SCI^+	CSI^-	$PCAES^+$	$PBMF^+$	WLI^-
1	4	4	4	3	4	2	4	2	4	4	5
2	5	5	5	5	5	5	6	2	5	3	5
3	5	5	6	5	6	5	6	5	5	5	6
4	6	6	3	6	5	6	6	6	5	6	6
5	4	4	3	4	4	6	6	4	6	5	6

Table 1.11 Actual cluster number decided by CVI's

Data set ID	1	2	3	4	5
Possible cluster values	2^2 3 5 4^7	2^2 3 5^7 6	5^7 6^4	3 5^2 6^8	3 4^5 5 6^4
Chosen cluster value	4	5	5	6	4

1.4 Conclusion

The FCM algorithm when coupled with the firefly optimization generates promising results for medical image segmentation. After the removal of medical image film artifacts, denoising of input image was performed by NLTD filtering approach prior to segmentation and the computation complexity was minimized by the optimal pixel count selection. The Firefly optimization based improved FCM generates satisfactory and consistent results with FCM-Cuckoo, FCM-ABC and FCM-SA segmentation techniques. The few parameter tuning of firefly optimization makes it a robust choice for image processing applications. A detailed analysis of cluster validity performance metrics were also done for the appropriate determination of number of clusters.

This work highlights the importance of optimization algorithms in image segmentation. The FCM is a widely used clustering segmentation technique, however to solve the issues in FCM, numerous algorithms like SFCM, ARKFCM, FLICM, T2FCM etc. have been proposed. But the above-mentioned techniques are concentrating mainly on the performance of FCM when the input images are noisy. The optimization techniques are then employed in FCM for solving the problem of random centroid initialization, but the tuning of parameters and computation complexity generate issues. The novelty of the proposed work is as follows; the filtering was accomplished by NLTD filter which has good edge preservation, firefly optimization was employed which has fewer parameters to be tuned and has quick convergence rate. The outcome of this work will provide a path for the researchers to develop novel optimization algorithm for solving the problems in image processing.

Acknowledgements The authors would like to acknowledge the support provided by DST under IDP scheme (No: IDP/MED/03/2015). We thank Dr. Sebastian Varghese (Consultant Radiologist, Metro Scans & Laboratory, Trivandrum) for providing the medical CT images and supporting us in the preparation of the manuscript.

References

1. Fida, B., Bernabucci, I., Bibbo, D., Conforto, S., Schmid, M.: Pre-processing effect on the accuracy of event-based activity segmentation and classification through inertial sensors. Sensors **15**(9), 23095–23109 (2015)
2. Hemanth, D.J., Anitha, J.: Image pre-processing and feature extraction techniques for magnetic resonance brain image analysis. In: Computer Applications for Communication, Networking, and Digital Contents, pp. 349–356. Springer, Berlin (2012)
3. Lee, L.K., Liew, S.C., Thong, W.J.: A review of image segmentation methodologies in medical image. In: Advanced Computer and Communication Engineering Technology, pp. 1069–1080. Springer, Cham (2015)
4. Kumar, S.N., Muthukumar, S., Kumar, A., Varghese, S.: A voyage on medical image segmentation algorithms. Biomed. Res. (2018)
5. Sharma, N., Aggarwal, L.M.: Automated medical image segmentation techniques. J. Med. Phys. Assoc. Med. Physicists India **35**(1), 3 (2010)
6. Banerjee, S., Mitra, S., Shankar, B.U.: Single seed delineation of brain tumor using multi-thresholding. Inf. Sci. **10**(330), 88–103 (2016)
7. Smistad, E., Elster, A.C., Lindseth, F.: GPU accelerated segmentation and centerline extraction of tubular structures from medical images. Int. J. Comput. Assist. Radiol. Surg. **9** (4), 561–575 (2014)
8. Pal, S.K., Rosenfeld, A.: Image enhancement, and thresholding by optimization of fuzzy compactness. Pattern Recogn. Lett. **7**(2), 77–86 (1988)
9. Li, M., Yan, J.H., Li, G., Zhao, J.: Self-adaptive Canny operator edge detection technique. J. Harbin Eng. Univ. **9**(28) (2007)
10. Günsel, B., Jain, A.K., Panayirci, E.: Reconstruction and boundary detection of range and intensity images using multiscale MRF representations. Comput. Vis. Image Underst. **63**(2), 353–366 (1996)
11. Thirumavalavan, S., Jayaraman, S.: An improved teaching-learning based robust edge detection algorithm for noisy images. J. Adv. Res. **7**(6), 979–989 (2016)
12. Zhao, F., Xie, X.: An overview of interactive medical image segmentation. Ann. BMVA **2013** (7), 1–22 (2013)
13. Senthilnath, J., Omkar, S.N., Mani, V.: Clustering using firefly algorithm: performance study. Swarm Evol. Comput. **1**(3), 164–171 (2011)
14. Fister, I., Fister Jr., I., Yang, X.S., Brest, J.: A comprehensive review of firefly algorithms. Swarm Evol. Comput. **1**(13), 34–46 (2013)
15. Wang, H., Zhou, X., Sun, H., Yu, X., Zhao, J., Zhang, H., Cui, L.: Firefly algorithm with adaptive control parameters. Soft. Comput. **21**(17), 5091–5102 (2017)
16. Alsmadi, M.K.: A hybrid firefly algorithm with Fuzzy-C mean algorithm for MRI brain segmentation. Am. J. Appl. Sci. **11**(9), 1676–1691 (2014)
17. Vennila, K., Thamizhmaran, K.: Multilevel image segmentation based on firefly algorithm. Biometrics Bioinform. **9**(3), 57–60 (2017)
18. Selvaraj, C., Kumar, R.S., Karnan, M.: A survey on application of bio-inspired algorithms. Int. J. Comput. Sci. Inf. Technol. **5**(1), 366–370 (2014)
19. Nayak, J., Naik, B., Behera, H.S.: Fuzzy C-means (FCM) clustering algorithm: a decade review from 2000 to 2014. In: Computational Intelligence in Data Mining, vol. 2, pp. 133–149. Springer, New Delhi (2015)

20. Nayak, J., Nanda, M., Nayak, K., Naik, B., Behera, H.S.: An improved firefly fuzzy c-means (FAFCM) algorithm for clustering real-world data sets. In: Advanced Computing, Networking and Informatics, vol. 1, pp. 339–348. Springer, Cham (2014)
21. Lai, C.C., Chang, C.Y.: A hierarchical evolutionary algorithm for automatic medical image segmentation. Expert Syst. Appl. **36**(1), 248–259 (2009)
22. Hancer, E., Ozturk, C., Karaboga, D.: Extraction of brain tumors from MRI images with artificial bee colony based segmentation methodology. In: 2013 8th International Conference on Electrical and Electronics Engineering (ELECO), 28 Nov 2013, pp. 516–520. IEEE (2013)
23. Mirghasemi, S., Rayudu, R., Zhang, M.: A heuristic solution for noisy image segmentation using particle swarm optimization and fuzzy clustering. In: 2015 7th International Joint Conference on Computational Intelligence (IJCCI), 12 Nov 2015, vol. 1, pp. 17–27. IEEE (2015)
24. Moeskops, P., Viergever, M.A., Mendrik, A.M., de Vries, L.S., Benders, M.J., Išgum, I.: Automatic segmentation of MR brain images with a convolutional neural network. IEEE Trans. Med. Imaging **35**(5), 1252–1261 (2016)
25. Pereira, S., Pinto, A., Alves, V., Silva, C.A.: Brain tumor segmentation using convolutional neural networks in MRI images. IEEE Trans. Med. Imaging **35**(5), 1240–1251 (2016)
26. Liu, F., Jang, H., Kijowski, R., Bradshaw, T., McMillan, A.B.: Deep learning MR imaging-based attenuation correction for PET/MR imaging. Radiology **286**(2), 676–684 (2017)
27. Avendi, M.R., Kheradvar, A., Jafarkhani, H.: A combined deep-learning and deformable model approach to fully automatic segmentation of the left ventricle in cardiac MRI. Med. Image Anal. **30**, 108–119 (2016)
28. Liu, F., Zhou, Z., Jang, H., Samsonov, A., Zhao, G., Kijowski, R.: Deep convolutional neural network and 3D deformable approach for tissue segmentation in musculoskeletal magnetic resonance imaging. Magn. Reson. Med. **79**, 2379 (2017)
29. Badrinarayanan, V., Kendall, A., Cipolla, R.: Segnet: a deep convolutional encoder-decoder architecture for image segmentation. IEEE Trans. Pattern Anal. Mach. Intell. **39**(12), 2481–2495 (2017)
30. Dunn, J.C.: A fuzzy relative of the ISODATA process and its use in detecting compact well-separated clusters. J. Cybern. **3**, 32–57 (1973)
31. Hathaway, R.J., Bezdek, J.C.: Recent convergence results for the fuzzy c-means clustering algorithms. J. Classif. **5**(2), 237–247 (1988)
32. Yang, X.S.: Firefly algorithm, Levy flights and global optimization. In: Research and Development in Intelligent Systems, vol. XXVI, pp. 209–218. Springer, London (2010)
33. Roy, S., Bandyopadhyay, S.K.: Classification of brain disorder using medical imaging. Int. J. Curr. Med. Pharm. Res. **2**(11), 989–997 (2016)
34. Kumar, S.N., Fred, A.L., Kumar, H.A., Varghese, P.S.: Nonlinear tensor diffusion filter based marker-controlled watershed segmentation for CT/MR images. In: Proceedings of International Conference on Computational Intelligence and Data Engineering, pp. 317–331. Springer, Singapore (2018)
35. Wu, K.L., Yang, M.S.: A cluster validity index for fuzzy clustering. Pattern Recogn. Lett. **26** (9), 1275–1291 (2005)
36. Pal, N.R., Bezdek, J.C.: On cluster validity for the fuzzy c-means model. IEEE Trans. Fuzzy Syst. **3**(3), 370–379 (1995)
37. Kim, D.W., Lee, K.H., Lee, D.: Fuzzy cluster validation index based on inter-cluster proximity. Pattern Recogn. Lett. **24**(15), 2561–2574 (2003)
38. Wu, C.H., Ouyang, C.S., Chen, L.W., Lu, L.W.: A new fuzzy clustering validity index with a median factor for centroid-based clustering. IEEE Trans. Fuzzy Syst. **23**(3), 701–718 (2015)
39. Pakhira, M.K., Bandyopadhyay, S., Maulik, U.: Validity index for crisp and fuzzy clusters. Pattern Recogn. **37**(3), 487–501 (2004)
40. Chao, S.M., Tsai, D.M., Chiu, W.Y., Li, W.C.: Anisotropic diffusion-based detail-preserving smoothing for image restoration. In: 2010 17th IEEE International Conference on Image Processing (ICIP), 26 Sept 2010, pp. 4145–4148 (2010)

41. Ghazanfari, M., Alizadeh, S.: Learning FCM with Simulated Annealing. INTECH Open Access Publisher (2008)
42. Bose, A., Mali, K.: Fuzzy-based artificial bee colony optimization for gray image segmentation. SIViP **10**(6), 1089–1096 (2016)
43. Bhandari, A.K., Soni, V., Kumar, A., Singh, G.K.: Cuckoo search algorithm based satellite image contrast and brightness enhancement using DWT–SVD. ISA Trans. **53**(4), 1286–1296 (2014)
44. Katiyar, S., Patel, R., Arora, K.: Comparison and analysis of cuckoo search and firefly algorithm for image enhancement. In: International Conference on Smart Trends for Information Technology and Computer Communications, 6 Aug 2016, pp. 62–68. Springer, Singapore (2016)
45. Arora, S., Singh, S.: A conceptual comparison of firefly algorithm, bat algorithm, and cuckoo search. In: 2013 International Conference on Control Computing Communication & Materials (ICCCCM), 3 Aug 2013, pp. 1–4. IEEE (2013)
46. Yang, X.S., He, X.: Firefly algorithm: recent advances and applications. Int. J. Swarm Intell. **1** (1), 36–50 (2013)